

# From Modeling to Robust Control Design of Single-Mast Stacker Cranes

Sándor Hajdu<sup>\*</sup>, Péter Gáspár<sup>\*\*</sup>

<sup>\*</sup> Department of Mechanical Engineering, University of Debrecen  
Ótomető u. 2-4, H-4028 Debrecen, Hungary, e-mail: hajdusandor@eng.unideb.hu

<sup>\*\*</sup> Systems and Control Laboratory, Computer and Automation Research Institute,  
Hungarian Academy of Sciences  
Kende u. 13-17, H-1111 Budapest, Hungary, e-mail: gaspar.peter@sztaki.mta.hu

---

*Abstract: The paper presents the reduction of mast-vibration of single-mast stacker cranes by using a robust controller. During non-stationary movement undesirable mast vibrations may occur. These vibrations can reduce the positioning accuracy of the machine. The aim of this paper is to present the design procedure from the dynamic modeling to robust control design, in which accurate signal tracking and mast-vibration attenuation are guaranteed. The dynamic modeling of single-mast stacker cranes by means of multi-body modeling approach is summarized. The handling of varying dynamic behavior due to varying lifted load position is presented. For control design purposes the order of the model is reduced. Based on the modeling technique an appropriate robust  $H_\infty$  controller design method is applied. The trade-off between accurate reference signal tracking and mast-vibration attenuation is presented through demonstration example.*

*Keywords: robust  $H_\infty$  control; multi-body modeling; stacker cranes*

---

## 1 Introduction

In the last few decades warehouse technology has improved significantly and highly automated systems have appeared in this area. The essential elements in automated storage/retrieval systems (AS/RS) of warehouses are the stacker cranes, which perform directly the storage/retrieval operation into/from the rack position. The performance of automated storage/retrieval systems depends on the performance of stacker cranes. The advanced stacker cranes therefore must meet the fast working cycle and reliable, economical operation requirements. Thus these machines often have very high dynamic loads on their frame structures. The requirements of economical operation cause the reduction of the dead-weight of stacker crane frame structures. The reduction of dead-weight may result in decreasing the stiffness of the frame structure. Consequently, this structure is more

responsive to dynamic loads. During operation, therefore, undesirable, low-frequency and high-amplitude mast vibrations may occur in the frame structure due to the different inertial forces. The high-amplitude mast vibrations may reduce the stability and positioning accuracy of the stacker crane and in an extreme case they may damage the structure. A line drawing of a single-mast stacker crane with its main components is shown in Figure 1.

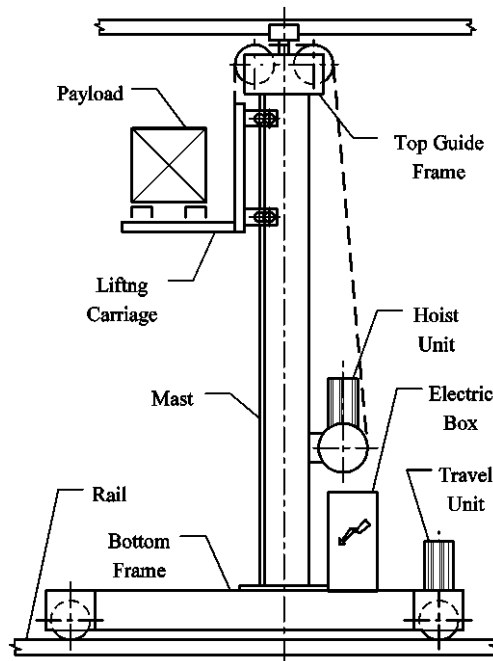


Figure 1  
Single mast stacker crane

For above-mentioned reasons it is necessary to reduce the undesirable mast vibrations by controlling the traveling motion of the stacker crane (i.e. the motion towards the aisle of the warehouse). In this paper a controller designing technique based on  $H_\infty$  approach is introduced. In the literature of stacker cranes only a few examples can be found concerning mast vibration attenuation by motion control (see e.g. [4-5]). Unfortunately these works do not take the effects of the lifted load position into account. The aim of the work is to introduce a controller design method which can handle the uncertainties in a dynamic model (e.g. varying lifted load positions and magnitudes) and at the same time it has good reference signal tracking and mast-vibration attenuation properties.

In the work the multi-body modeling approach is applied to describe the dynamic behavior of single-mast stacker cranes. It is a widely used method of structural dynamics and has a very extensive literature in the area of dynamic investigation

of engineering structures [7-10] as well as stacker cranes [1-6]. In our model structural damping is taken into consideration by means of the so-called proportional damping (Rayleigh damping) approach. The determination of the attributes of proportional damping is presented in detail by references [15-17]. The relatively high-order multi-body model is not suitable for  $H_\infty$  control design methods thus the investigated model is reduced with a suitable model order reduction method. Some dynamic model reduction methods are presented in references [12-14].

The paper is organized as follows: Section 2 introduces the control oriented dynamic modeling of single-mast stacker cranes through a multi-body modeling approach. The state space representation and the uncertainties of the model are also introduced. The model order reduction is also presented in Section 3. In Section 4 the robust control design problem is set and the solution method is presented. The operation of the designed control system is illustrated through simulation examples in Section 5.

## 2 Control-oriented Modeling of Single-Mast Stacker Cranes

In this section a linear dynamic model of single-mast stacker cranes is introduced, which is suitable for the representation of the dynamic behavior of stacker cranes under varying load conditions. For this purpose the Multi-body modeling technique is chosen. Besides finite element modeling (FEM) the multi-body modeling approach is one of the most frequently applied methods in dynamic analysis. The advantages of this method are the lower degree of freedom (compared with FEM) and simpler equations of motion. In addition favorable characteristic of this method is that the varying lifted load positions and magnitudes can be modeled in a very simple way.

The linear multi-body model of the stacker crane structure is presented in Fig. 2. In this model the mast structure (a box girder) is divided into sections between the lumped mass components of the stacker crane e.g. the bottom frame, the hoist unit, the top guide frame etc. The Euler-Bernoulli beam sections are approximated by lumped mass elements. These rigid elements are generated by the division of sections (with length  $l_i$ ) into  $N_i$  pieces. The lumped masses are located in the center of elements (in the so-called nodes). All inertia effects are concentrated at these nodes. The magnitudes of lumped masses are equal to the masses of corresponding beam pieces. The elements are interconnected by elastic but massless links. This elasticity approximates the bending elasticity of the original Euler-Bernoulli beams. The elasticity is provided by spiral springs (with spring stiffness  $S_{ei}$ ) connected parallel to the ideal, frictionless hinges. The magnitude of this spring stiffness is calculated by means of the strength of materials.

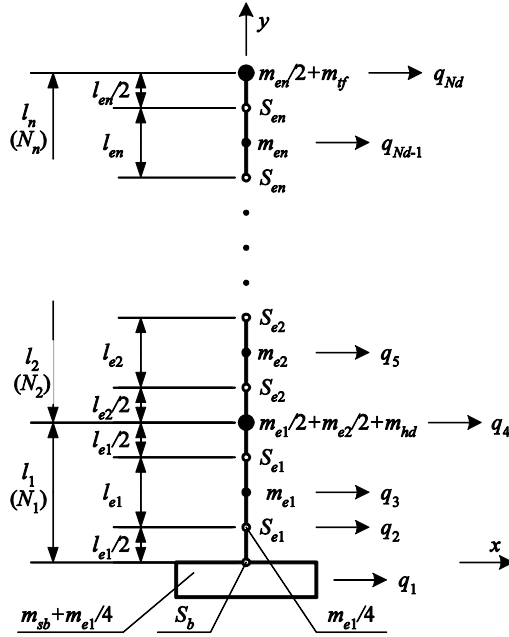


Figure 2  
Multi-body model of a single-mast stacker crane

As Figure 2 shows further components of a stacker crane are modeled by lumped masses i.e. the gross weight of the bottom frame (with idle and drive wheel blocks, the electric box, etc.), the masses of the hoist unit and the top guide frame. The mass of bottom the frame is denoted by  $m_{sb}$ , the mass of the hoist unit by  $m_{hd}$  and the mass of the top guide frame by  $m_y$ . The effect of the lifted load (the mass of payload and the lifting carriage) can be taken into consideration by means of adding its mass to the proper nodal mass. In this way the lifted load can be placed into discrete positions. The elasticity of the bottom frame beam is approximated by a spiral spring ( $S_b$ ) between the lumped mass of the bottom frame and the lower end of the mast.

In the generation of the motion equations of the multi-body model first the generalized coordinates must be selected. With the adequate selection of the generalized coordinates the mass and stiffness matrices of the motion equations can be transformed into a diagonal form. In this way the generation process of the motion equations can be simplified significantly. One of the possible choices of generalized coordinates (i.e. the  $q_i$  vertical displacement of each lumped mass) are shown in Figure 2. The degree of freedom (DOF) of the model is denoted by  $N_d$ .

The generalized coordinate vector of the model is:

$$\mathbf{q} = [q_1 \quad q_2 \quad \dots \quad q_{N_d}]^T \quad (1)$$

The differential equations of motion can be determined in several ways e.g. by means of using the Euler-Lagrange equations. The detailed derivation of mass and stiffness matrices and dynamic equations for the above-mentioned multi-body model can be found in [11]. The general form of the matrix equation of motion in the case of excited vibrations (i.e. in the presence of external excitation forces) is:

$$\mathbf{M}\ddot{\mathbf{q}} + \mathbf{D}\dot{\mathbf{q}} + \mathbf{S}\mathbf{q} = \mathbf{F}, \quad (2)$$

where  $\mathbf{M}$  is the mass matrix,  $\mathbf{S}$  is the stiffness matrix and  $\mathbf{D}$  is the damping matrix of the system. Here  $\mathbf{F}$  in general is the vector of external excitation forces. In this paper a single-input system is examined, where the input signal of our model is the external force acting in the direction of  $q_1$  generalized coordinate. Thus in vector  $\mathbf{F}$  only this coordinate has a value other than zero.

The input signal of the model is the external force acting in the direction of  $q_1$  generalized coordinate. In the following steps the model is applied in the synthesis of the controller which realizes the positioning control of single-mast stacker cranes. Therefore the outputs of the investigated state space representation can be classified into two groups. The first one is used for analyzing the mast-vibrations in arbitrary mast locations. These performance outputs are the inclinations of the mast i.e. the horizontal position difference between the lowest point of the mast and an arbitrary location of the mast. The second one is the measurement output, which is the horizontal position or velocity of the stacker. The state space realization of a linear time invariant system in general is described by the following equations.

$$\begin{aligned} \dot{\mathbf{x}} &= \mathbf{A}\mathbf{x} + \mathbf{B}_1\mathbf{d} + \mathbf{B}_2\mathbf{u}, \\ \mathbf{z} &= \mathbf{C}_1\mathbf{x} + \mathbf{D}_{11}\mathbf{d} + \mathbf{D}_{12}\mathbf{u}, \\ \mathbf{y} &= \mathbf{C}_2\mathbf{x} + \mathbf{D}_{21}\mathbf{d} \end{aligned} \quad (3)$$

where  $\mathbf{x}$ ,  $\mathbf{d}$ ,  $\mathbf{u}$  are the state vector, disturbance and control input respectively and  $\mathbf{x}_0 \in R^n$  is the initial state of the system. Here  $n$  is known as the number of the states and  $m$  and  $p$  are the number of input and output variables of the system respectively. Let us define the state vector with the generalized coordinate vector as follows:

$$\mathbf{x} = [\dot{\mathbf{q}} \ \mathbf{q}]^T. \quad (4)$$

For design of a robust controller model uncertainties also must be taken into account. Pokorádi in his paper [23] gives an overview of types and sources of model uncertainties and illustrates model uncertainty examination methods. Model uncertainties occur when some of the parameters in the investigated system are not precisely known, or can vary in a given range. The system can also have complex parameter variations satisfying a given magnitude bound. In this case uncertainty is modeled by connecting an unknown but bounded perturbation to the plant. Thus generally two kinds of uncertainty structures are used in the area of controller design i.e. structured and unstructured uncertainty models.

In simpler cases unstructured uncertainty models are used, which require only little information about model uncertainty i.e. the magnitude bound and the type of connection. The bounded perturbation can be connected to the plant in several ways, e.g. in additive, multiplicative, coprime factor uncertainty ways, etc.

In this case the two main sources of model uncertainty are the neglected dynamics due to model order reduction and the variation in load conditions. The dynamic properties, e.g. resonance frequencies, mode-shapes etc. of stacker cranes depend on the magnitude and position of the lifted load. The dynamic model must also take this effect into consideration. In order to solve this problem with the multi-body modeling technique a series of dynamic models are generated with varying lifted load magnitudes and heights. With this model set the variation in the dynamic behavior of stacker crane structures can be investigated. In order to take into consideration the properties of the entire model set in one model the variation of dynamic behavior is modeled as unstructured uncertainty.

From the several possible choices of connection types in this work the so-called output-multiplicative uncertainty model is applied. The formula of this uncertainty model is  $\mathbf{G}(s) = (\mathbf{I} + \mathbf{A}_m(s)\mathbf{W}_r(s))\mathbf{G}_N(s)$ , where  $\mathbf{G}(s)$  is the normalized uncertain neighborhood of the nominal system  $\mathbf{G}_N(s)$ ,  $\mathbf{A}_m(s)$  is unknown but bounded perturbation and  $\mathbf{W}_r(s)$  is a known weighting function, which reflects the amount of uncertainty. The bound of perturbation is defined as  $\|\mathbf{A}_m(s)\|_\infty < 1$ .

### 3 Model Order Reduction

The aim of this section is to find a suitable model order reduction method for this large degree of freedom system. In the literature several kinds of model order reduction methods can be found and an overview of these methods is presented in [14].

In the work the modal truncation (MT) method is analyzed, in which the reduced order model is derived by truncating a state space transformation as follows:  $(\mathbf{A}, \mathbf{B}, \mathbf{C}, \mathbf{D}) \rightarrow (\mathbf{T}\mathbf{A}\mathbf{T}^{-1}, \mathbf{T}\mathbf{B}, \mathbf{C}\mathbf{T}^{-1}, \mathbf{D})$ , where  $\mathbf{T} \in \mathbb{R}^{n \times n}$  is a nonsingular transformation matrix. The purpose of the MT method is to project the dynamics of original model onto an  $\mathbf{A}$ -invariant subspace corresponding to the dominant modes of the system. These dominant modes can be selected by eigenvalues of  $\mathbf{A}$  (i.e. the poles of  $\mathbf{G}$ ). The selection of the dominant modes plays an important role since the accuracy of approximation is determined by these modes. In this case the first two eigenvalues (with the smallest absolute value) correspond to the rigid body motion of the stacker crane, which must be kept in the reduced model. Further dominant vibratory modes corresponding to the next three complex conjugate eigenvalue-pairs are also involved in the reduced model. This way the

accuracy of the reduced model in the relevant frequency range will be acceptable. Thus, the order of reduced model in this case is eight.

The transformation matrices of MT can be computed by means of the following considerations. Let us assume that  $A$  is assumed to be diagonalizable by the help of transformation matrix  $T$ , where the columns of  $T$  are the eigenvectors ( $t_j, j=1..n$ ) of  $A$ . Thus the state space representation can be projected onto an  $A$ -invariant subspace spanned by the  $r$  pieces of most dominant eigenvectors. The following partition of the transformation matrix  $T$ :  $T^{-1} = [\tilde{T}_l \ \tilde{L}_l]^T, \tilde{T}_l \in R^{n \times r}$  using  $T_l^T = \tilde{T}_l (T_r^T \tilde{T}_l)^{-1}, T_l \in R^{r \times n}$  and  $T = [T_r \ L_r], T_r \in R^{n \times r}$ . The matrices of the reduced order model can be calculated by the following truncation:  $T^{-1}AT = \begin{bmatrix} \hat{A} & 0 \\ 0 & A_2 \end{bmatrix}, T^{-1}B = \begin{bmatrix} \hat{B} \\ B_2 \end{bmatrix}, CT = [\hat{C} \ C_2]$ . The error bound of this method is calculated as:

$$\|G - \hat{G}\|_{\infty} \leq \|C_2\| \|B_2\| \frac{1}{\min_{\lambda \in \Lambda(A_2)} |\operatorname{Re}(\lambda)|}. \quad (5)$$

The Bode magnitude diagrams of original and reduced systems corresponding to the two outputs are shown in Figure 3 a) while the absolute errors between the original and the reduced models are presented in Figure 3 b).

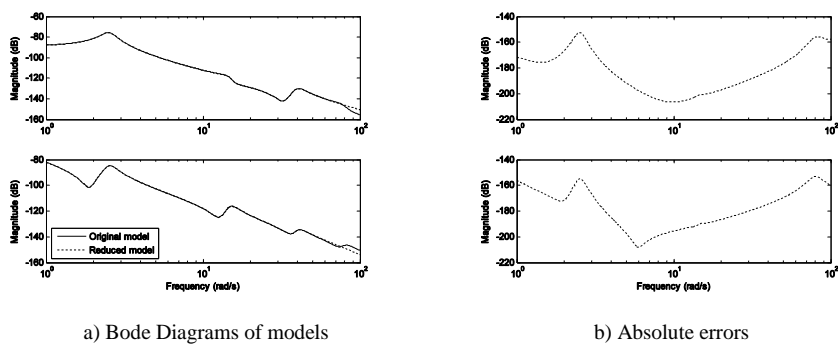


Figure 3  
Results of model order reduction

## 4 Robust Control Design

For purpose of controller design the so-called  $H_{\infty}$  method is chosen. The main motivation behind this choice is that this method allows taking the model uncertainties into account. In an actual controller design setup the performance objectives of controller design are expressed by means of weighting functions.

The weighting functions can be considered as penalty functions, i.e. weights should be large in the frequency range where small signals are desired and small where large performance outputs can be tolerated. The control objectives i.e. the weighting strategy of controller design are presented in Figure 4.

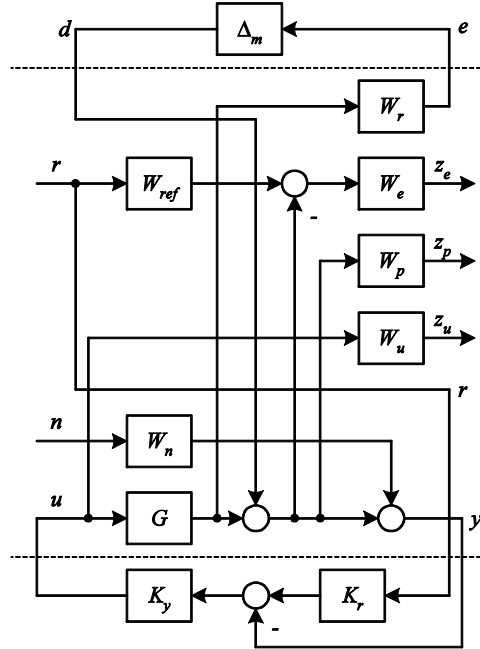


Figure 4

The robust  $H_\infty$  controller design setup

The most important requirements for the closed-loop system are good reference signal tracking property and mast-vibration attenuation. The reference signal in the investigated model is the horizontal position demand of the stacker crane. The good reference signal tracking performance objective can be formulated by means of the two-degree-of-freedom controller structure. In this structure the controller  $\mathbf{K}$  is partitioned into two parts:  $\mathbf{K}_y$  and  $\mathbf{K}_r$ . Here  $\mathbf{K}_y$  is the feedback part of the controller while  $\mathbf{K}_r$  is the pre-filter part. The ideal model of the closed-loop system is represented by the transfer function  $W_{ref}$ .

Usually this function is a second-order transfer function with free parameters  $\omega$  and  $\zeta$ :

$$W_{ref} = \frac{\omega_r^2}{s^2 + 2\zeta\omega_r s + \omega_r^2}. \quad (6)$$

This way the bandwidth and the damping of the ideal closed-loop transfer function can be adjusted. The error between the ideal and the actual closed-loop transfer function is weighted by the penalty function  $W_e$ . Usually a more accurate model is desired in the low frequency range thus  $W_e$  is a low-pass filter:

$$W_e = A_e \frac{1 + T_{en}s}{1 + T_{ed}s}, \quad (7)$$

where  $\omega_{en} = 1/T_{en} > \omega_{ed} = 1/T_{ed}$ .

The above mentioned two-degree-of-freedom controller is placed on the second (position) output of the stacker crane model. This provides for good reference signal tracking properties of the positioning control of the stacker crane. The mast-vibrations are penalized by the  $W_p$  weighting function, which acts on the first (mast inclination) output of stacker crane model. Since the steady-state value of mast inclination must not be penalized, the  $W_e$  transfer function is a high-pass filter:

$$W_p = A_p \frac{1 + T_{pn}s}{1 + T_{pd}s}, \quad (8)$$

where  $\omega_{pn} = 1/T_{pn} < \omega_{pd} = 1/T_{pd}$ .

The control input is limited by using the performance criteria  $W_u$ . With this weight larger control signals can be penalized and thereby the control activity can be minimized. This way the undesired hysteresis effect in the actuator system can be avoided. The transfer function  $W_u$ , similarly, to the transfer function  $W_e$  is a high-pass filter with parameters  $A_u$ ,  $\omega_{un}$  and  $\omega_{ud}$ . The purpose of the weighting function  $W_n$  is to reflect the sensor noises. This function is also a high-pass filter with parameters  $A_n$ ,  $\omega_{nn}$  and  $\omega_{nd}$ . The parameters of this function can be determined from experiments or manufacturer measurements of the actual sensor system.

The robust controller can be calculated the so-called  $H_\infty/\mu$  synthesis which is based on the following optimization problem:

$$\min_{\mathbf{K}} \mu_{\mathcal{A}}[F_l(\mathbf{P}, \mathbf{K})], \quad (9)$$

where  $\mu_{\mathcal{A}}$  is a matrix function called the structured singular value (SSV). The symbol  $F_l(\mathbf{P}, \mathbf{K})$  denotes the lower linear fractional transformation (LFT) of the augmented plant  $\mathbf{P}$  and controller  $\mathbf{K}$ . The exact definition of  $\mu_{\mathcal{A}}$  and LFT can be found in e.g. [18-21].

The direct computation of  $\mu_{\mathcal{A}}$  is intractable. Thus, bounds on the SSV are typically used in place of the actual SSV during robust performance analysis. The following optimization problem provides a tight upper bound on the SSV and can be reliably computed.

$$\min_{\mathbf{K}} \inf_{\mathbf{D}, \mathbf{D}^{-1} \in H_\infty} \bar{\sigma}(\mathbf{D}F_l(\mathbf{P}, \mathbf{K})\mathbf{D}^{-1}). \quad (10)$$

The stable and minimum phase scaling matrix  $\mathbf{D}$  is chosen such that  $\mathbf{D}\mathbf{A} = \mathbf{A}\mathbf{D}$ . The optimization problem can be solved iteratively for  $\mathbf{K}$  and  $\mathbf{D}$ . This is the so-called  $\mathbf{D} - \mathbf{K}$  iteration, see [21].

For a fixed scaling transfer matrix  $\mathbf{D}$

$$\min_{\mathbf{K}} \|\mathbf{D}F_l(\mathbf{P}, \mathbf{K})\mathbf{D}^{-1}\|_\infty \quad (11)$$

is a standard  $H_\infty$  optimization problem. For a given stabilizing controller  $\mathbf{K}$

$$\inf_{\mathbf{D}, \mathbf{D}^{-1} \in H_\infty} \|\mathbf{D}F_l(\mathbf{P}, \mathbf{K})\mathbf{D}^{-1}\|_\infty \quad (12)$$

is a standard convex optimization problem and it can be solved iteratively pointwise in the frequency domain:  $\sup_\omega \inf_{\mathbf{D}_\omega \in \mathbf{D}} \bar{\sigma}(\mathbf{D}_\omega F_l(\mathbf{P}, \mathbf{K})(j\omega)\mathbf{D}_\omega^{-1})$ .

## 5 Demonstrational Example

In this section a design case study is presented with two kinds of weighting strategy. The main parameters of the stacker crane are shown in Table 1. In the investigations the lifted load position varies in the position range from 41 *m* to 44 *m*, which generates the model uncertainty. The nominal model of this model set is the one with a lifted load position in the middle of the position range, i.e., 42.5 *m*.

The matrix of uncertainty weighting functions is presented in the Bode diagrams of Figure 5. These functions are 4<sup>th</sup> order approximation functions of the relative errors in the investigated model set. In these diagrams the amount of multiplicative uncertainty is relatively low due to the limited load position range. This uncertainty value increases sharply only in the frequency ranges surrounding the natural frequencies.

The model matching function i.e. the ideal model of the closed-loop system is given by  $W_{ref} = \frac{8^2}{s^2 + 16s + 8^2}$ . The first weighting strategy (Case #1) focuses the

reference signal tracking rather than the mast-vibration attenuation. While in the second strategy (Case #2) the mast-vibrations are penalized more heavily. The  $W_e$  and  $W_p$  performance weighting functions in the first and the second weighting strategy are presented in the Bode diagrams of Figure 6.

Table 1  
Main parameters of investigated stacker crane

Denomination	Denotation	Value
Payload:	$m_p$	1200 kg
Mass of lifting carriage:	$m_{lc}$	410 kg
Mass of hoist unit:	$m_{hd}$	470 kg
Mass of top guide frame:	$m_{gf}$	70 kg
Mass of bottom frame:	$m_{sb}$	2418 kg
Lifted load position:	$h_h$	1-44 m
Length of mast-sections:	$l_1$	3,5 m
	$l_2$	11,5 m
	$l_3$	30 m
Cross-sectional areas of mast-sections:	$A_1; A_2$	0,02058 m <sup>2</sup>
	$A_3$	0,01518 m <sup>2</sup>
Second moments of areas:	$I_{z1}; I_{z2}$	0,00177 m <sup>4</sup>
	$I_{z3}$	0,00106 m <sup>4</sup>

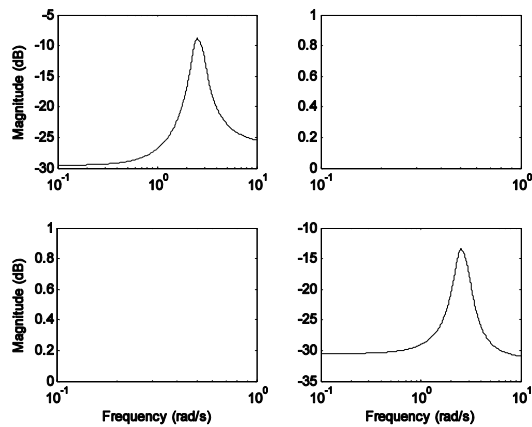


Figure 5  
Uncertainty weighing function matrix

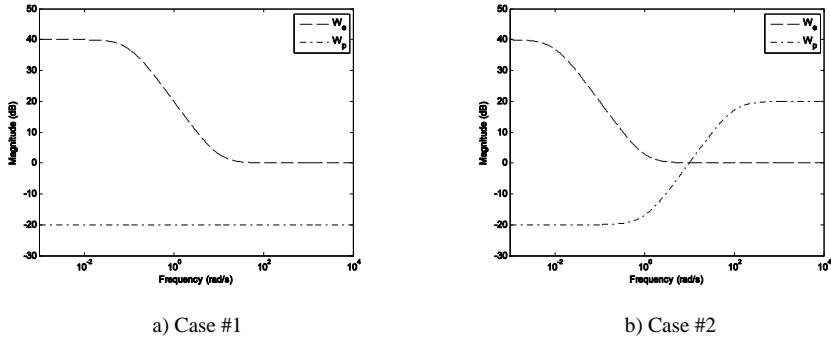


Figure 6  
Performance weighting functions  $W_e$  and  $W_p$

The weighting functions of control input and sensor noises are presented in Figure 7 a) and b). These functions are the same in both design cases.

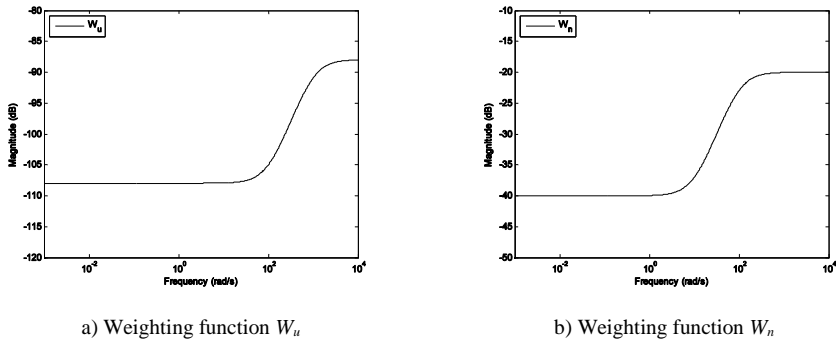
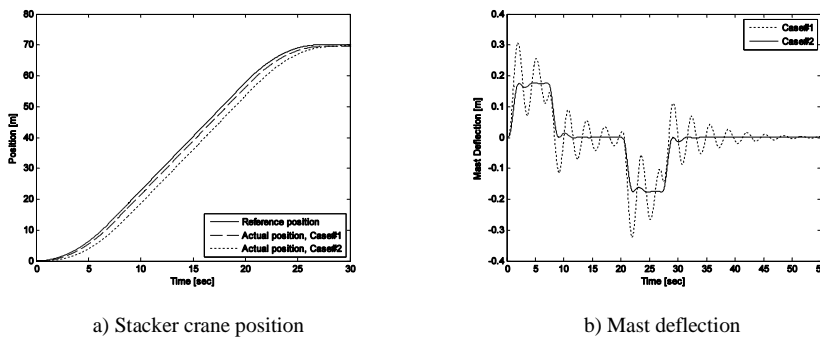


Figure 7  
Control input and sensor noises weighting functions

The validation of the designed controllers can be carried out in the time domain analysis. In this simulation the position signal of a general stacker crane moving cycle is used as reference signal. In the first session of the moving cycle the stacker crane has constant  $0,5 \text{ m/s}^2$  desired acceleration. In the second session the desired velocity is  $3,5 \text{ m/s}$  and the deceleration value of the third session is  $-0,5 \text{ m/s}^2$ . The distance covered during the moving cycle is  $70 \text{ m}$  while the total cycle time is 27 seconds. The simulation results, i.e., diagrams of the stacker crane position and mast deflection are shown in Figure 8.



a) Stacker crane position

b) Mast deflection

Figure 8

Simulation results

The simulation results show the trade-off between mast-vibration attenuation and the cycle time of stacker crane motion. With the controller of the first case the closed-loop system produces adequate reference signal tracking properties in addition to relatively high mast-vibrations. However, with the second design the mast vibrations are attenuated significantly but the cycle time of stacker crane motion increased by approximately 1.5 seconds.

## Conclusions

In the paper a controller design method has been presented which can handle the uncertainties in the dynamic model and at the same time it has good reference signal tracking and mast-vibration attenuation properties. The first part of this paper summarizes the dynamic modeling of single-mast stacker cranes by means of the multi body modeling approach. The unstructured uncertainty approach is applied to handle varying dynamic behaviors due to varying lifted load positions. An  $H_\infty$  controller design method is proposed, which is suitable for the positioning control of stacker cranes with reduced mast vibrations in the presence of model uncertainties. In a demonstrational example the trade-off between mast vibration attenuation and the cycle time of stacker crane motion is also presented. The design method is suitable for finding the controller which produces the desired motion cycle time and/or mast-vibration free stacker crane motion.

## References

- [1] Arnold, D., Schumacher, M., Optimierung frdertechnischer Komponenten unter dynamischen Belastungen, *F+H Frdern und Heben* 43, 1993, Nr. 1-2, pp. 18-25
- [2] Reisinger, K. H., *Schwingungssimulation von Regalfrderzeugen*, Dissertation, Technische Universitt Graz, 1998
- [3] Schumacher, M., *Untersuchung des Schwingungsverhaltens von Einmast-Regalbediengerten*, Dissertation, Institut fr Frdertechnik Karlsruhe, 1994, pp. 11-24

- 
- [4] Arnold, D., Dietzel, M., Aktive Schwingungsdämpfung von Regalbediengeräten, *F+H Fördern und Heben* 50, 2000, Nr. 1-2, pp. 50-52
- [5] Dietzel, M., *Beeinflussung des Schwingungsverhaltens von Regalbediengeräten durch Regelung des Fahrantriebs*, Dissertation, Institut für Fördertechnik Karlsruhe, 1999
- [6] Köhne, M., Analyse und Modellierung des dynamischen Verhaltens von Regalbediengeräten, *VDI-Berichte*, Issue 1756, 2003, pp. 1039-1048
- [7] Jalón, J. G., Bayo, E., *Kinematic and Dynamic Simulation of Multibody Systems. The Real-Time Challenge*, Springer-Verlag, New-York, 1994
- [8] Angeles, J., Kecskeméthy, A., *Kinematics and Dynamics of Multi-Body Systems*, Springer-Verlag, New York, 1995
- [9] Keskinen, E., Kuokkala, V-T., Vuoristo, T., Martikainen, M., Multi-Body Wave Analysis of Axially Elastic Rod Systems, *Proc. IMechE*, Vol. 221 Part K: J. Multi-body Dynamics, 2007
- [10] Ziaei-Rad, S., Ariaei, A., Imregun, M., Vibration Analysis of Timoshenko Beams under Uniform Partially Distributed Moving Masses, *Proc. IMechE*, Vol. 221 Part K: J. Multi-body Dynamics, 2007
- [11] Hajdu, S., Gáspár, P., Investigation of the Influence of Lifted Load on Dynamic Behavior of Stacker Cranes through Unstructured Uncertainties, *CINTI 2013 : Proceeding of the 14<sup>th</sup> IEEE International Symposium on Computational Intelligence and Informatics*, 2013, pp. 179-184
- [12] Benner P., Quintana-Ortí E. S., Quintana-Ortí G., State-Space Truncation Methods for Parallel Model Reduction of Large-Scale Systems, *Parallel Computing - Special issue: Parallel and distributed scientific and engineering computing*, Volume 29, Issues 11-12, 2003, pp. 1701-1722
- [13] Nowakowski, C., Kürschner, P., Eberhard, P., Benner, P., Model Reduction of an Elastic Crankshaft for Elastic Multibody Simulations, *ZAMM - Journal of Applied Mathematics and Mechanics*, Volume 93, Issues 4, 2013, pp. 198-216
- [14] Dukic, S. D., Saric, A. T., Dynamic Model Reduction: An Overview of Available Techniques with Application to Power Systems, *Serbian Journal of Electrical Engineering*, Volume 9, Issue 2, 2012, pp. 131-169
- [15] Spears, R. E., Jensen, S. R., Approach for Selection of Rayleigh Damping Parameters Used for Time History Analysis, *ASME Pressure Vessels and Piping Division Conference*, Prague, 2009
- [16] Chowdhury, I., Dasgupta, S., Computation of Rayleigh Damping Coefficients for Large Systems, *The Electronic Journal of Geotechnical Engineering*, Vol. 8, 2003

- 
- [17] Pápai, F., Adhikari, S., Wang, B., Estimation of Modal Dampings for Unmeasured Modes, *Slovak Journal of Civil Engineering* 20:4, 2012, pp. 1-11
- [18] Balas, G., Chiang, R., Packard, A., Safonov, M., *Robust Control Toolbox 3 User's Guide*, The MathWorks, Inc., 2007
- [19] Doyle, J. C., Glover, K., Khargonekar, P. P., Francis, B. A., State Space Solutions to Standard  $H_2$  and  $H_\infty$  Control Problems, *IEEE Trans. Automatic Control* Vol. AC-34, 1989, No. 8, pp. 831-837
- [20] Zhou, K., Doyle, J. C., *Essentials of Robust Control*, Prentice Hall, New Jersey, 1998
- [21] Zhou, K., Doyle, J. C., Glover, K., *Robust and Optimal Control*, Prentice Hall, New Jersey, 1996
- [22] Balas, G., *Robust Control of Flexible Structures: Theory and Experiments*, PhD. Thesis, California Institute of Technology, 1990
- [23] Pokorádi, L., Uncertainties of Engineering Simulation, *Proceedings of International Conference on Innovative Technologies IN-TECH 2010*, Prague, Czech Republic, 2010, pp. 121-124